[12] Y. Murakami, I. Hatakeyama, and H. Tsuchiya, "Normalized frequency dependence of splice losses in single-mode optical fibers," *Electron. Lett.*, vol. 18, no. 9, pp. 277–278, 1978.
[13] M. Tateda, S. Tanaka, and Y. Sugiyama, "Thermal characteristics of phase shift in jacketed optical fibers," *Appl. Opt.*, vol. 19, no. 5, pp. 770–773, 1980.
[14] N. Lagakos, J. A. Bucaro, and J. Jarzynski, "Temperature-induced optical phase shifts in fibers," *Appl. Opt.*, vol. 20, no. 13, pp. 2305–2308, 1981.
[15] H. S. Carslaw and J. C. Jager, *Conduction of Heat in Solids*, 2nd ed. Oxford: Clarendon, 1959, p. 230.
[16] G. B. Hocker, "Fiber-optic acoustic sensors with composite structures: An analysis," *Appl. Opt.*, vol. 18, no. 21, pp. 3674–3683, 1979.
[17] B. Budiansky, D. C. Drucker, G. S. Kino, and J. R. Rice, "Pressure sensitivity of a clad optical fiber," *Appl. Opt.*, vol. 18, no. 24, pp. 4085–4088, 1979.

Toshihiko Yoshino was born in Tokyo, Japan, on April 27, 1939. He received the B.S., M.S., and Ph.D. degrees in applied physics from Tokyo University, Tokyo, Japan, in 1963, 1965, and 1968, respectively.

Since 1968 he has been with the Institute of Industrial Science, Tokyo University, where he has been engaged in research and education on optics. From 1971 to 1973 he was a Guest Researcher with the Technical University, Hannover, West Germany, where he worked on laser spectroscopy.

Dr. Yoshino is a member of the Japan Society of Applied Physics.

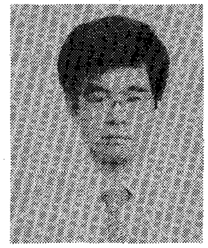

Kiyoshi Kurosawa was born in Nagano Prefecture, Japan, on September 6, 1952. He received the B.E. degree in electrical engineering from Nihon University, Tokyo, Japan, in 1978 and graduated from the Department of Technology, University Course, Tokyo Electric Power Institute, Tokyo, Japan, in 1980.

Since 1971 he has been with the Tokyo Electric Power Corporation, Ltd., Tokyo, Japan, where he has been engaged in research and development in application of optics in electric power systems.

Katsuji Itoh was born in Tokyo, Japan, on February 15, 1942. He received the B.S. and the M.S. degrees in electrical engineering from the Yokohama National University, Yokohama, Japan, in 1966 and 1968, respectively.

Since 1968 he has been with the Furukawa Electric Corporation, Ltd., Chiba, Japan, where he has been engaged in research and development in distribution and application of optics to high voltage

Mr. Itoh is a member of the Institute of Electrical Engineers of Japan and the Japan Society of Applied Physics.

Teruzi Ose, photograph and biography not available at the time of publication.

Microbend Fiber-Optic Sensor as Extended Hydrophone

NICHOLAS LAGAKOS, W. J. TROTT, T. R. HICKMAN, JAMES H. COLE, AND JOSEPH A. BUCARO

Abstract—**A novel microbend fiber-optic acoustic sensor has been studied, both analytically and experimentally. The sensor is simple mechanically, insensitive to acceleration, and achieves shape flexibility by utilizing fairly long fiber lengths for the sensing element. The acoustic sensitivity and minimum detectable pressure of the sensor were found to be significantly improved over previously reported microbend sensors. Further optimization of the sensor appears possible.**

I. Introduction

INTENSITY modulation induced by microbending in multimode fibers has been utilized as a transduction mechanism for acoustic [1] and displacement [2] sensors with promising results. Such sensors are based on intensity modulation of core [1] or clad [2] modes produced by a periodic axial deformation of the fiber. In the original sensors of this type a short section (1-3 cm) of a multimode fiber is deformed periodically by a pair of corrugated pieces called a deformer. The mechanical design of these sensors is rather complicated, the alignment of the deformer is critical, the sensor bandwidth is limited, and acceleration effects can deteriorate the sensor performance.

In order to avoid these problems, the novel microbend sensor described in this paper was designed and tested. The sensor is simple mechanically, free of acceleration effects, and utilizes much longer fiber lengths as the sensing element, thus providing some shape flexibility. In addition, the sensor has a significantly improved acoustic performance over those previously reported.

Below, we report our analytic and experimental study of the acoustic sensitivity and threshold detectability of the sensor. We also discuss the principles involved in the acoustical and optical optimization of such sensors.

Manuscript received March 16, 1982; revised May 12, 1982.
The authors are with the Acoustics Division, Naval Research Laboratory, Washington, DC 20375.

II. Acoustooptic Transduction by Microbending

Periodic axial deformation of an optical fiber will cause mode coupling which redistributes the light power among core modes and couples core-to-clad modes. It is possible to configure fibers in such a way that applied pressure produces axial deformation. If this is done, an acoustic wave can be detected by monitoring the light power in the core [1] or clad [2] modes. Such an intensity-modulated microbend fiber-optic sensor is shown schematically in Fig. 1. Light from a source such as a laser or a light emitting diode is coupled into a multimode fiber and propagates through an acoustically sensitive section of the fiber (sensing element).

Let $W_o T$ be the light power incident on the detector, where T is the total optical power transmission coefficient through the acoustic sensor, and W_o is the input light power to the sensing element. When an acoustic pressure Δp is applied to the sensor, the transmission coefficient will change by ΔT and the detector signal current i_s is given by the following expression [3]:

$$i_s = \frac{qeW_o}{h\nu}\left(\frac{\Delta T}{\Delta p}\right)\Delta p \tag{1}$$

where q is the quantum efficiency of the detector, h is Planck's constant, ν is the light frequency, and $\Delta T/\Delta p$ is the transduction coefficient of the sensor.

The mean-square shot noise current in the detector is given by [4]

$$i_N^2 = 2e\left(\frac{qe}{h\nu}\right) W_o T\,\Delta f \tag{2}$$

where Δf is the detection bandwidth. The minimum detectable pressure, assuming a shot-noise limit sensor, can be found by equating the signal and noise currents, which gives

$$p_{\min} = \left(\frac{2Th\nu\Delta f}{qW_o}\right)^{1/2}\left(\frac{\Delta T}{\Delta p}\right)^{-1}. \tag{3}$$

The transduction coefficient of the sensor $\Delta T/\Delta p$ can be written as

$$\frac{\Delta T}{\Delta p} = \left(\frac{\Delta T}{\Delta X}\right)\left(\frac{\Delta X}{\Delta p}\right). \tag{4}$$

Here, ΔX is the change in the amplitude of the fiber deformation. In (4) $\Delta T/\Delta X$ depends on the sensitivity of the optical fiber to microbending losses, and $\Delta X/\Delta p$ depends on the acoustical and mechanical design of the sensor.

A. Microbend Loss

Since the early days of fiber optics, the optical loss due to microbending has deliberatively been minimized. What is required for sensing is an optical fiber having just the opposite characteristics, leading to a high $\Delta T/\Delta X$. Besides intrinsic fiber parameters such as numerical aperture, core/cladding thickness, etc. [5], the periodicity of the fiber deformation is an important parameter in determining $\Delta T/\Delta X$. In order to understand this dependence, let us consider briefly the mode coupling effect in fibers.

The theory of mode coupling has been studied extensively [6]-[9]. It has been shown theoretically [8] and proven experimentally [10] that when a periodic microbend is induced along the fiber axis, light power is coupled between modes with longitudinal propagation constants k and k' satisfying

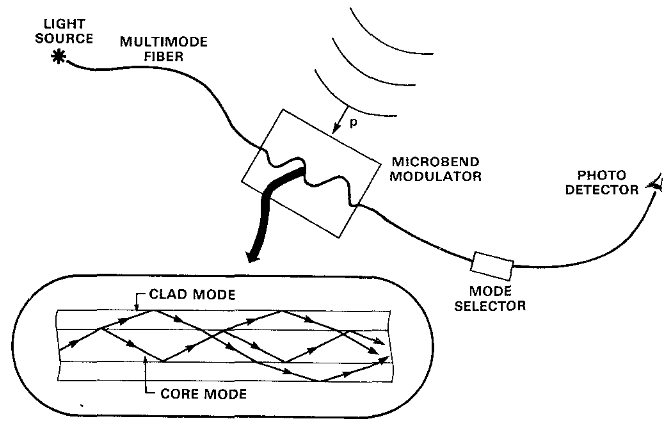

Fig. 1. Microbend fiber-optic acoustic sensor. Insert: pressure induced mode coupling.

$$k - k' = \pm\frac{2\pi}{\Lambda} \tag{5}$$

where Λ is the mechanical wavelength of the periodic perturbation.

A useful form for the refractive index profile of a fiber is [11]

$$n^2(r) = n^2(0)[1 - 2\Delta(r/a)^{\alpha}] \tag{6}$$

where $\Delta = [n^2(0) - n^2(a)]/2n^2(0)$. Here, $n(0)$, $n(r)$, and $n(a)$ are the refractive indexes at distances $0, r$, and a from the fiber axis, respectively, a is the core radius and α is a constant. A step profile corresponds to $\alpha = \infty$. Applying the WKB approximation [12] to the solution of the dielectric waveguide problem [11], [12] it can be shown that the wave number separation of neighboring modes is given for the profile (6) by [13]

$$k_{m+1} - k_m = \left(\frac{\alpha}{\alpha+2}\right)\frac{2\sqrt{\Delta}}{a}\left(\frac{m}{M}\right)^{[\alpha-2/\alpha+2]} \tag{7}$$

where m is the modal group label and M is the number of modal groups. For step index fibers, (7) becomes

$$k_{m+1} - k_m = \frac{2\Delta^{1/2}}{a}\left(\frac{m}{M}\right). \tag{8}$$

From (5) and (8) we can calculate the periodicity required to switch neighboring modes. These values are shown qualitatively in Fig. 2, and as can be seen, high-order modes (large m) are coupled with small Λ, while low-order modes (small m) are coupled with large Λ.

Therefore, when the microbend transduction is based on the coupling of core to radiated modes, high sensitivity is expected only with periodicities which couple the highest order core modes to radiated modes. These periodicities can be approximately obtained from (5) and (8) with $m = M$

$$\Lambda_c = \frac{\pi a}{\Delta^{1/2}}. \tag{9}$$

B. Mechanical Considerations

Having discussed the optical loss term $(\Delta T/\Delta X)$ in (4), we now consider the mechanical factor $(\Delta X/\Delta p)$. In most microbend sensors, pressure is applied to the fiber indirectly through acoustic couplers (pistons, diaphragms, etc.) which are used as

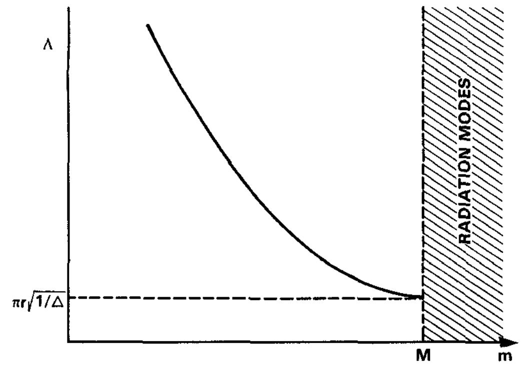

Fig. 2. Required periodicity for coupling neighboring core modes (8) versus mode order in a step index multimode fiber.

pressure multipliers. If A is the area of the acoustic coupler against which the acoustic pressure is applied, (4) can be written as follows:

$$\frac{\Delta T}{\Delta p} = \left(\frac{\Delta T}{\Delta X}\right)(AC_m) \tag{10}$$

where C_m is the mechanical compliance of the sensor. The term AC_m in (10) depends on the sensor design. The mechanical complicance of the sensor will later be found from the equivalent acoustic circuit of the sensor. When the compliance of the surrounding fluid is substantially larger than the mechanical compliance of the sensing element C_f, the compliance of the sensor C_m is approximately equal to C_f

$$C_m \simeq C_f = G\frac{\Lambda^3}{Ed^4}\frac{1}{n} \tag{11}$$

where d is the diameter of the fiber, E is Young's modulus of the fiber, n is the number of the deformer intervals, and G is a constant which depends on how the fiber is loaded and suspended.

From (1), (10), and (11) we see that high sensitivity is obtained with a large deformer periodicity Λ and small values of E, d, and n. However, Young's modulus E of typical glasses used for optical fibers does not vary much, certainly not by an order of magnitude. Also, very small values of d are prevented due to light coupling and fiber mechanical strength considerations. Finally, even though lowering the number of deformer intervals n increases C_f, it decreases $\Delta T/\Delta X$ by the same amount. Thus, for fixed A the sensor sensitivity is approximately independent of n. In practice, the optimum value of n is determined from mechanical design considerations such as the desired frequency of the sensor mechanical resonance. The sensor resonance is due to the mass-spring relationship of the fiber and the acoustic coupler.

III. Microbend Hydrophone Design Using Extended Sensing Element

The fiber used in the present microbend hydrophone was a step index, aluminum coated, multimode fiber with a 0.133 numerical aperture, made by Hughes Research Laboratory. The fiber consisted of a 60 μm OD core of 95 percent SiO_2-4 percent GeO_2-1 percent P_2O_5, a 125 μm OD cladding of 95 percent SiO_2-5 percent B_2O_3, and a 165 μm OD aluminum coating [14]. The microbending sensitivity, $\Delta T/\Delta X$ of this fiber was first studied experimentally as a function of applied force F and mechanical periodicity Λ. A 5 cm fiber section was sandwiched between two circular plates with parallel corrugations and force was applied to one of these plates. The periodicity was varied by rotating the fiber against the plates and using plates with different periodicities. Fig. 3 shows $\Delta T/\Delta F$ versus periodicity for this fiber at a force of $1N$. Using (10) and (12) the microbending sensitivity $\Delta T/\Delta X$ was then obtained from $\Delta T/\Delta F$ in terms of the mechanical compliance of the fiber C_f, which for a bar loaded at the center and clamped at its ends, is given by the following expression [15]:

$$C_f = \frac{\Lambda^3}{3\pi Ed^4 n}. \tag{12}$$

Fig. 4 shows $\Delta T/\Delta X$ versus Λ for a force of $1N$. As can be seen from this figure, the microbending sensitivity exhibits a very strong peak at ~1.5 mm. This is in agreement with the prediction of Λ_c = 1.45 mm of (9) with a = 30 μm and Δ = 0.0042 (NA = 0.133, n_o = 1.458). This periodicity couples the highest order modes to radiated modes. The microbending sensitivity decreases very rapidly as the periodicity increases (Fig. 4), since long periodicities couple low-order modes only (9), resulting in smaller losses in transmission through the fiber. However, the sensitivity of the sensor is proportional to $\Delta T/\Delta F$ (Fig. 3) which, in turn, is proportional to $\Delta T/\Delta X$ weighted by Λ^3 (12). The net result is to increase the sensitivity at long periodicities. In practice, these long periodicities are preferred since toroids (Fig. 5) with small precisely determined periodicities are harder to realize. For the actual sensor construction, a 5.5 mm periodicity was chosen. Such a periodicity can couple only relatively low-order neighboring modes, which were monitored in these experiments to obtain maximum sensitivity.

Fig. 5 shows schematically the design of our spacially extended hydrophone. A 6.24 m length of fiber is wrapped around a 3.6 cm OD aluminum tube in a machined thread (Fig. 5, insert). The fiber is exposed to the sound pressure periodically in axial slots that cut below the root of the thread. A rubber boot encloses the tube and the fiber, so that the fiber within the thread regions and outside the slots is not in contact with the boot and thus is unexposed to the sound field. The rubber boot, which is in contact with the fiber within the axial slots, is the acoustic coupler through which the applied pressure deflects the fiber sinusoidally. In Fig. 6, upper part, the fiber is shown as a circumferential wrap periodically supported. The sound pressure p is applied only over half of the circumference and deflects the fiber inwards. The portion of the fiber that is isolated from the sound field is deflected in the opposite direction by a force moment at the fiber supports, i.e., the edges of the axial slots. For operation at depth, the static pressure response must be eliminated. This can be achieved by means of a capillary hole which connects the air surrounding the fiber to the air inside the aluminum tube, where the equivalent of an accumulator is installed. For operation at extreme depths, liquid must be substituted for air and a small port should be utilized as a low-pass filter to equalize the hydrostatic pressure inside and outside the aluminum tube.

In order to predict the sensitivity [(1) and (4)] and the minimum detectable pressure (3) of the sensor, the sensor mechanical compliance C_m must be found in terms of the mechanical compliance of the fiber. This can be done from the equivalent circuit of the sensor for one microbend interval, which is shown in the lower part of Fig. 6. In this figure p is the applied

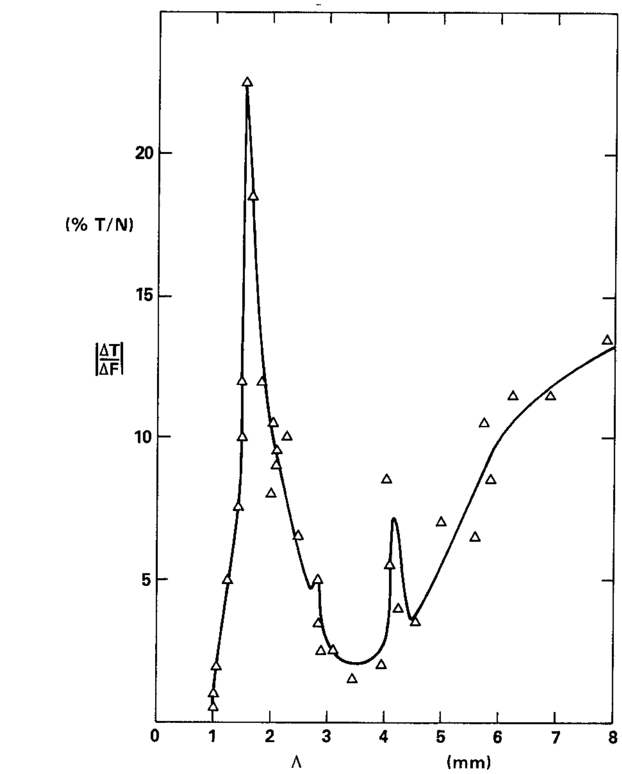

Fig. 3. Experimentally obtained $\Delta T/\Delta F$ versus periodicity (triangles) for the Hughes Research Laboratory step index aluminum coated fiber. Solid line: eye fit.

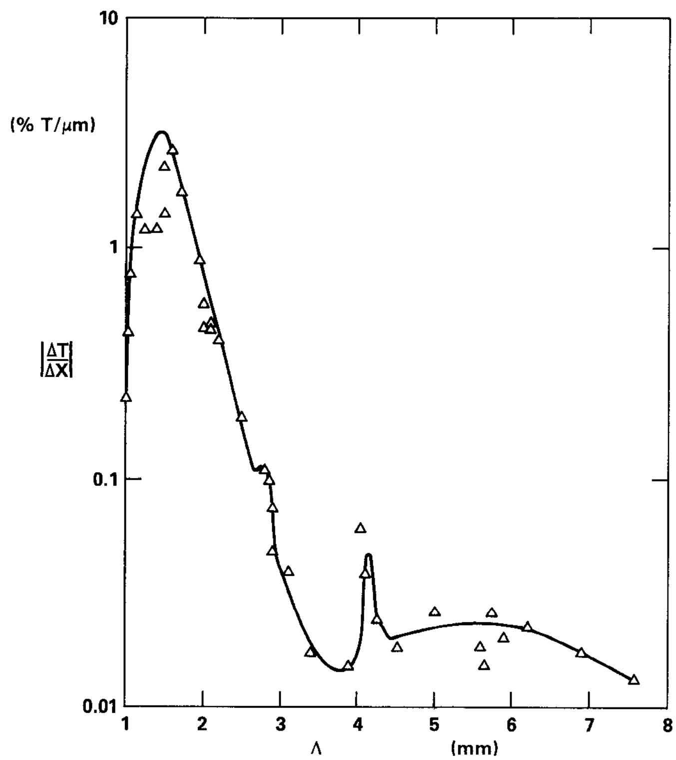

Fig. 4. Microbending sensitivity $\Delta T/\Delta X$ versus periodicity (triangles) for the aluminum coated fiber.

pressure, C_{A1} and C_{A2} are the acoustic compliances ($A'^2 x$ mechanical compliance, A' being the area per periodic interval) of the exposed and unexposed portions of the fiber, C_{A_r} is the acoustic compliance of the rubber tube, m_{A1} and m_{A2} are the acoustic masses (mechanical masses/A'^2) of the exposed and unexposed portions of the fiber, respectively, and m_r is the effective acoustic mass of the rubber tube plus a radiation reactance mass. For the sensor reported here, the compliance of the rubber tube C_A is much larger than that of the bent fiber and, therefore, can be ignored. Assuming that the fiber deflection in the exposed and unexposed section are equal, we get $C_{A2} = C_{A1}$. From Fig. 6, lower part, we can see that the effective acoustic compliance C_A' of the sensor per periodic interval can be expressed as follows:

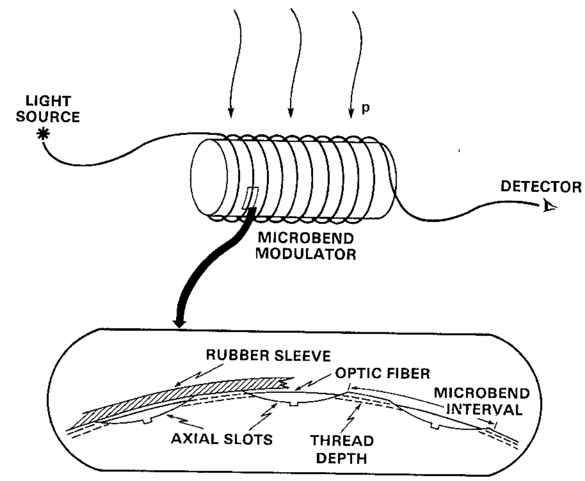

Fig. 5. Extended microbend acoustooptic sensor.

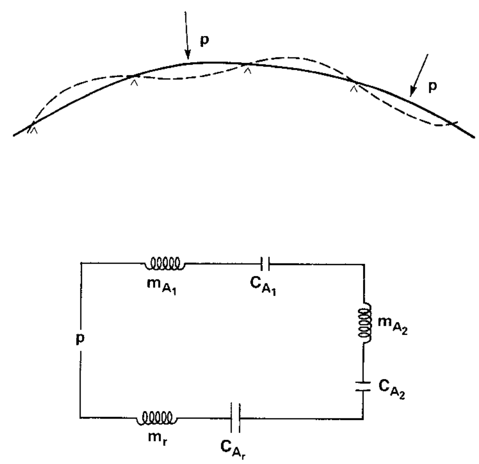

Fig. 6. Upper: two periodic fiber intervals of the extended hydrophone. Lower: equivalent acoustic circuit of one interval.

$$\frac{1}{C_A'} = \frac{1}{C_{A1}} + \frac{1}{C_{A2}} = \frac{2}{C_{A1}}. \tag{13}$$

Treating the fiber as a freely supported bar, it can be shown [16] that, for uniform loading, the mechanical compliance over one interval is given by

$$C_{f'} = C_{A_1}/A'^2 = \frac{5}{6}\frac{(\Lambda/2)^3}{\pi E d^4}. \tag{14}$$

The total acoustic compliance of the sensor with n periodic intervals is

$$C_A = C_A'/n. \tag{15}$$

The total area A is $A'n$. Thus, the product AC_m in (10) is independent of the number of periodic intervals

$$AC_m = A'C'_m \cong A'C'_f. \tag{16}$$

The resonance of the hydrophone ω_o is determined from the following equation:

$$\omega_o = \frac{1}{m_A C'_A} \tag{17}$$

where $m_A = m_{A1} + m_{A2} + m_r$, as can be seen from Fig. 6. The frequency response of the sensor is expected to be flat from a low frequency to about one octave below the sensor resonant frequency $f_o (= \omega_o / 2\pi)$.

IV. Hydrophone Measurements and Discussion

The acoustic response of the spatially extended hydrophone was measured in the following manner. Light emitted from a very low-noise single mode 100 Tropel laser at 0.6328 μm of ~1 mW power was coupled into the fiber with a 20X microscope objective which insured a fill aperture. Light in the clad modes was stripped just before the detector and light power of the core modes was detected by a p-i-n photodiode. Acoustic signals were generated in an acoustic calibrator consisting of an open-ended column of water excited by an electrodynamic drive. The pressure distribution in such a system is uniform horizontally and has only a small vertical gradient. A standard calibrated hydrophone was inserted at the level of the fiber coil and was used to measure the acoustic pressure levels.

Fig. 7 shows the measured frequency response of the hydrophone sensitivity from 200 to 1500 Hz (triangles). As can be seen from this figure, the sensitivity is approximately −215 dB re 1 V/μPa, is flat to within ±1 dB, and substantially better than those reported previously (circles) [17]. Using the analysis of the previous section, the sensitivity of the hydrophone per fiber bend is predicted to be −255 dB re 1 V/μPa. Assuming a linear dependence of bend loss with sensing element length l, the sensitivity of our hydrophone having 1134 periods is expected to be −194 dB re 1 V/μPa which is 21 dB higher than that obtained experimentally (Fig. 7). This difference was found to be due to coupling of clad modes back to core modes. Such a coupling results in a weaker than linear $\Delta T/\Delta X$ versus length dependence. Indeed, subsequent measurements of the sensitivity $\Delta T/\Delta X$ of this aluminum coated fiber as a function of the length of the sensing element demonstrated that

$$\frac{\Delta T}{\Delta X} \propto l^q \tag{18}$$

where $q = 0.737$. When the less than linear dependence on length is taken into account, the predicted sensitivity is within 5 dB of that measured. This indicates that in order to obtain the full sensitivity from long lengths of sensing elements, care must be taken to prevent coupling of clad modes back to core modes, which can be done, for example, by using highly absorbing coatings. Indeed, we have since demonstrated this experimentally on moderate lengths of fibers painted with oil-based paint where we found $\Delta T/\Delta X \propto l$.

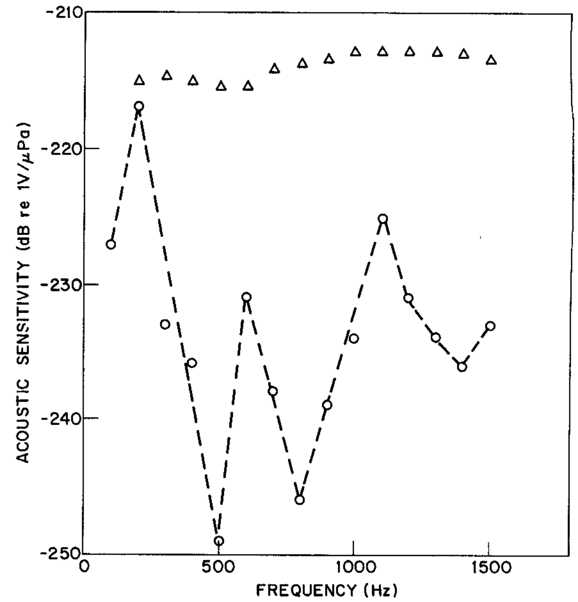

Fig. 7. Frequency response of the sensitivity of the present extended hydrophone (triangles) and the microbend hydrophone of [17] (circles).

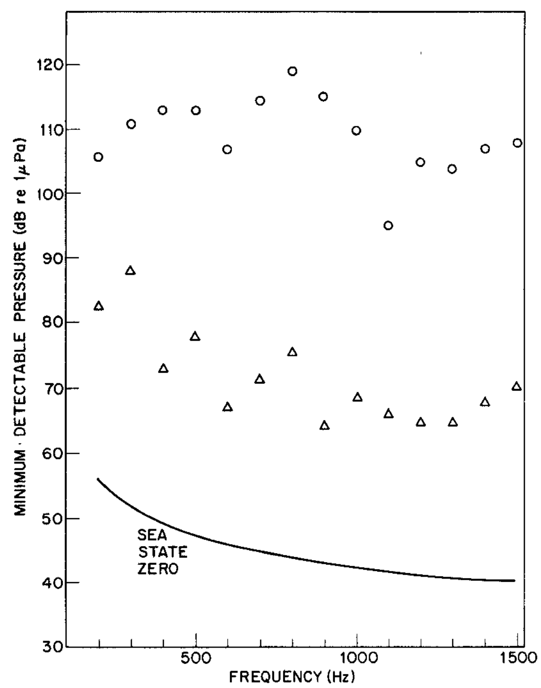

Fig. 8. Frequency response of the minimum detectable pressure of the extended hydrophone (triangles) and the microbend hydrophone of [18] (circles). Solid line: sea state zero.

Fig. 8 shows the minimum detectable pressure of the extended hydrophone (triangles) and the previously reported microbend sensor (circles) [18] from 200 to 1500 Hz. The solid line shows the standard noise reference for sea state zero. As can be seen from this figure, for frequencies higher than 500 Hz, the minimum detectable pressure of 70 dB re 1 μPa is only about 25 dB higher than the sea state zero, a significant improvement over that of the previously reported microbend sensor [18]. This minimum detectable pressure is about 20 dB higher than that predicted from (3), (10), and

(18) (with $q = 1$), which is consistent with the lower than expected sensitivity. At frequencies below 500 Hz, the electronic noise of the laser significantly deteriorates the sensor minimum detectable pressure.

This detectability compares favorably with those of other intensity devices [19]. Although evanescent [20], Schlieren [21], and photoelastic [22] sensors have all demonstrated thresholds about 10 dB lower than reported here, additional optimization of the microbend sensor is practical. For example, increased optical power or fiber length could provide added sensitivity.

Finally, the resonance of the extended hydrophone was calculated from (17) to be about 30 kHz, much higher than that of previous microbend hydrophones [17].

V. Conclusion

A novel microbend fiber-optic acoustic sensor has been studied both analytically and experimentally. The sensor is simple mechanically, acceleration insensitive, and utilizes long fiber lengths as a sensing element providing shape flexibility. The sensor was found to have a broad bandwidth and an acoustic sensitivity and threshold detectability significantly improved over previously reported microbend sensors. The results here also indicate that long fibers can be utilized as the sensing element to achieve increased acoustic performance if the conversion of clad modes back to core modes is prevented.

References

[1] J. N. Fields, C. K. Asawa, C. P. Smith, and R. J. Morrison, "Fiber-optic hydrophone," in *Physics of Fibers, Vol. 2, Advances in Ceramics*, B. Bendow and S. S. Mitra, Eds. American Ceramic Society, 1981, pp. 529–538.

[2] N. Lagakos, T. Litovitz, P. Macedo, R. Mohr, and R. Meister, "Multimode optical fiber displacement sensor," *Appl. Opt.*, vol. 20, pp. 167–168, 1981.

[3] J. N. Fields, C. P. Smith, C. K. Asawa, R. J. Morrison, O. G. Ramer, G. L. Tangonan, and M. K. Barnoski, in *Conf. Proc. Opt. Fiber Commun.*, Washington, DC, Mar. 6–8, 1979, pp. 58–59; also J. N. Fields, C. K. Asawa, O. G. Ramer, and M. K. Barnoski, "Fiber optic pressure sensor," *J. Acoust. Soc. Amer.*, vol. 67, pp. 816–818, 1980.

[4] A. Yariv, *Introduction to Optical Electronics.* New York: Holt, Rinehart, and Winston, 1971, p. 254.

[5] C. M. Miller, "Laminated fiber ribbon for optical communication cables," *Bell Syst. Tech. J.*, vol. 55, pp. 929–935, 1976.

[6] D. Gloge, "Optical power flow in multimode fibers," *Bell Syst. Tech. J.*, vol. 51, pp. 1767–1783, 1972.

[7] D. Marcuse, *Theory of Dielectric Optical Waveguides.* New York: Academic, 1974.

[8] D. B. Keck, *Fundamentals of Optical Fiber Communications*, M. Barnoski, Ed. New York: Academic, 1976.

[9] J. E. Widwinter, *Optical Fibers for Transmission.* New York: Wiley, 1979.

[10] L. Jeunhomme and J. P. Pocholle, "Mode coupling in a multimode optical fiber with microbends," *Appl. Opt.*, vol. 14, pp. 2400–2405, 1975.

[11] D. Gloge and E. A. J. Marcatili, "Multimode theory of graded-core fibers," *Bell Syst. Tech. J.*, vol. 52, pp. 1563–1578, 1973.

[12] E. Merzbacker, *Quantum Mechanics.* New York: Wiley, 1961.

[13] C. N. Kurtz and W. Streifer, *IEEE Trans. Microwave Theory Tech.*, vol. MTT-17, p. 250, 1969.

[14] N. Lagakos, T. R. Hickman, J. H. Cole, and J. A. Bucaro, "Optical fibers with reduced pressure sensitivity," *Opt. Lett.*, vol. 6, pp. 443–445, 1981.

[15] F. L. Singer, *Strength of Materials.* New York: Harper and Brothers, 1962, 2nd ed., p. 265.

[16] F. L. Singer, *Strength of Materials.* New York: Harper and Brothers, 1962, 2nd ed., p. 235.

[17] Unpublished data of hydrophone reported in [18].

[18] J. N. Fields and J. Cole, "Fiber microbend acoustic sensor," *Appl. Opt.*, vol. 19, pp. 3265–3267, 1980.

[19] J. H. Cole, N. Lagakos, and J. A. Bucaro, "Advances in fiber optic based acoustic sensors," presented at SPIE Meet., Los Angeles, CA, Jan. 1982.

[20] J. D. Beasley, "Multimode optical evanescent-wave acoustic sensor," *J. Acoust. Soc. Amer.*, vol. 68, pp. 595–598, 1980.

[21] W. B. Spillman, Jr. and D. H. McMahon, "Schlieren multimode fiber-optic hydrophone," *Appl. Phys. Lett.*, vol. 37, pp. 145–147, 1980.

[22] ——, "Multimode fiber optic hydrophone based upon the photoelastic effect," *Appl. Opt.*, to be published.

Nicholas Lagakos, for a photograph and biography, see p. 535 of the April 1982 issue of this Transactions.

W. J. Trott, photograph and biography not available at the time of publication.

T. R. Hickman, photograph and biography not available at the time of publication.

James H. Cole, for a photograph and biography, see p. 511 of the April 1982 issue of this Transactions.

Joseph A. Bucaro, for a photograph and biography, see p. 511 of the April 1982 issue of this Transactions.